Experimental Neurology 338 (2021) 113603

Contents lists available at ScienceDirect

Experimental Neurology

journal homepage: www.elsevier.com/locate/yexnr

Research paper

Adult glut3 homozygous null mice survive to demonstrate neural excitability and altered neurobehavioral responses reminiscent of neurodevelopmental disorders

Bo-Chul Shin [a], Carlos Cepeda [b], Mason Eghbali [a], Shin Yun Byun [a], Michael S. Levine [b], Sherin U. Devaskar [a,*]

[a] Departments of Pediatrics, Division of Neonatology & Developmental Biology, The Neonatal Research Center of the UCLA Children's Discovery & Innovation Institute, David Geffen School of Medicine at UCLA, Los Angeles, CA 90095-1752, United States of America
[b] Intellectual and Developmental Disabilities Research Center and Brain Research Institute, David Geffen School of Medicine at UCLA, Los Angeles, CA 90095-1752, United States of America

ARTICLE INFO

Keywords:
Glutamate-excitatory neurons
Neurodevelopmental disorders
Loss-of-function polymorphisms
Seizure activity

ABSTRACT

Since GLUT3 is vital for fueling neurotransmission, we examined in-vivo the adult phenotype carrying the conditional homozygous *glut3* gene mutation (KO) in glutamate-excitatory neurons. These KO mice demonstrated sex-specific differences in brain and body weights ($p = 0.0001$ and $p = 0.01$ each) with reduced GLUT3 protein in cerebral cortices and brain stem ($p = 0.005$). In patch clamp studies the glut3 KO mice displayed a shorter latency to and enhanced paroxysmal activity ($p = 0.01$ and $p = 0.015$ each) in pyramidal neurons upon application of a $GABA_A$ antagonist, supporting hyperexcitability. Further, associated changes in neurobehavior consisted of reduced latency to fall in the rotorod motor test related to incoordination, increased distance traveled in total and periphery versus center in open field testing suggesting hyperactivity with anxiety ($p = 0.0013$ in male, $p = 0.045$ in female), reduced time freezing reminiscent of disrupted contextual fear conditioning ($p = 0.0033$), decreased time in target quadrant seen with spatial cognitive memory water maze testing ($p = 0.034$), and enhanced sociability particularly for novelty reflecting a lack of inhibition/impulsivity ($p = 0.038$). Some of these features were equally pronounced in males and females (cognitive) while others were seen in females (anxiety and impulsivity). We conclude that GLUT3 in adult glutamate-excitatory neurons is essential for maintaining neurotransmitory equipoise regulating excitation with maintenance of motor coordination and activity, cognition, spatial memory and normal fear for both contextual events and novelty with tempered sociability. While sex-specificity was forthcoming for some of these behaviors, our findings collectively suggest that loss-of-function glut3 gene mutations or polymorphisms may underlie an endophenotype of attention deficit-hyperactivity disorder.

1. Introduction

Glucose is an essential substrate for brain energy metabolism (Devaskar et al., 1992; Devaskar et al., 1999; Magistretti and Pellerin, 1999), a lack of which causes major neurological deficits (Dworschak et al., 2015; Roeske et al., 2011; Shah et al., 2012; Szablewski, 2017). Glucose is transported across the blood-brain barrier by a process of facilitated diffusion mainly mediated by glucose transporter isoform 1 (GLUT1) (Takata et al., 1997; Uldry and Thorens, 2004). Clinically, mutations of the GLUT1 gene have led to the GLUT1 deficiency syndrome (G1DS) which presents with major neurological deficits in patients with this disorder surviving into adult life (Leen et al., 2013; Pearson et al., 2013; Wang et al., 2005). Once glucose traverses the blood-brain barrier and enters the interstitial space, it crosses the cell membranes of glial (astrocytes, oligodendrocytes), microglial and neuronal cells fueling the production of ATP necessary for various cellular processes. While GLUT1 and GLUT5 facilitate glucose transport into glial and microglial components respectively, GLUT3 is the major neuronal glucose transporter.

Clinically, GLUT3 activating polymorphisms have been associated

* Corresponding author at: 10833 Le Conte Avenue, MDCC-22-412, Los Angeles, CA 90095-1752, United States of America.
E-mail address: Sdevaskar@mednet.ucla.edu (S.U. Devaskar).

https://doi.org/10.1016/j.expneurol.2021.113603
Received 10 September 2020; Received in revised form 5 January 2021; Accepted 9 January 2021
Available online 19 January 2021

with attention deficit-hyperactivity disorder (ADHD) in children and adults (Merker et al., 2017) while loss-of-function mutations have been seen in infants presenting with meningomyeloceles (Connealy et al., 2014), dyslexia and other neurodevelopmental disorders (Dworschak et al., 2015; Roeske et al., 2011), and offering protection against the inflammatory disorder of rheumatoid arthritis (Veal et al., 2014), which of recent may be controversial (Ziegler et al., 2020). To investigate the functional relevance of neuronal GLUT3, in-vitro investigations revealed a protective function against excitotoxicity, mediating neurotransmission via AMPK (Weisova et al., 2009). Studies in-vivo utilizing rodent/murine models revealed an adaptive incremental response of GLUT3 to hypoxic-ischemic injury (Devaskar et al., 1999; Zovein et al., 2004). Genetic mutation of glut3 demonstrated a loss of this adaptive response to hypoxic-ischemia in heterozygous null adults culminating in clinical seizures (Fung et al., 2010) and neurobehavioral aberrations under normal normoxic conditions (Zhao et al., 2010). However, survival of the homozygous counterpart beyond early embryonic life posed a challenge, since GLUT3 is expressed in the trophoectoderm as well (Carayannopoulos et al., 2014; Ganguly et al., 2007). Employing conditional tissue-specific strategies, we previously demonstrated postnatal survival of the nestin-CRE X *floxed* glut3 homozygous mice, that carried a frame-shift mutation in exon 6 thereby lacking neural GLUT3 expression. However, these mice also suffered early demise, making it difficult to fully examine the adult phenotype (Shin et al., 2018). Given that the lack of GLUT3 both in-vitro (Weisova et al., 2009) and in-vivo (Shin et al., 2018) caused a phenotype involving excitatory neurotransmission, we specifically mutated glut3 in glutamate-expressing pyramidal neurons by mating *Emx-1*-CRE mice with floxed glut3 mice, and examined the adult phenotypic presentation to gain further mechanistic insights as proof-of-principle. This strategy took advantage of *Emx-1* a nuclear transcription factor that plays a role in developmental patterning of the brain (Stocker and O'Leary, 2016) and subsequently is predominantly expressed in glutamate expressing excitatory pyramidal neurons (Chan et al., 2001).

2. Materials and methods

2.1. Creation and genotyping of glut3$^{flox/flox/Cre+}$ mice

2.1.1. Glut3$^{flox/flox/Emx1\text{-}Cre+}$

Glut3$^{flox/+}$ mice were generated on C57BL/6 background by inserting LoxP sites into introns 5 and 6 (Mouse Biology Program, University of California, Davis). We crossed male glut3$^{flox/+}$ mice with female glut3$^{flox/+}$ mice generating glut3$^{flox/flox}$ mice as previously described (Shin et al., 2018). For generation of glut3$^{flox/flox/Cre+}$ by Cre/loxP recombination, we next crossed glut3$^{flox/flox}$ mice with transgenic mice that expressed *Cre* recombinase under the regulation of an *Emx1* promoter, namely *Emx1-Cre* mice (B6.Cg-Tg[Emx1-cre]1Kln/J; Jackson Laboratory, USA), thereby creating *glut3*$^{flox/+/Emx1\text{-}Cre+}$ mice. Subsequently, mating male glut3$^{flox/+/Emx1\text{-}Cre+}$ mice with female glut3$^{flox/+/Emx1\text{-}Cre+}$ mice generated glut3$^{flox/flox/Emx1\text{-}Cre+}$ mice. Finally, female glut3$^{flox/flox}$ mice were crossed with male glut3$^{flox/\ flox\ /Emx1\text{-}Cre+}$ mice, generating the glut3 conditional knockout (KO) mice designated as glut3$^{flox/flox/Emx1\text{-}Cre+}$ (homozygous KO). Since glut3$^{flox/flox}$ without *Cre* in preliminary studies expressed a phenotype no different from the wild type (*wt*, glut3$^{+/+}$) despite the introduction of *loxP* sites in two intronic regions, glut3$^{flox/flox}$ served as the control (CON) genotype for our subsequent studies as previously described (Shin et al., 2018).

2.1.2. Genotyping of conditional glut3 deleted mouse lines

By polymerase chain reaction (PCR) upon analysis of mouse tail DNA samples, the presence of glut3$^{flox/flox}$ presented as a 402 bp DNA fragment which served as control without the presence of *Cre*, while the absence of glut3$^{flox/flox}$, namely wild type for the glut3 gene (glut3$^{+/+}$ which is not *floxed*) produced a 233 bp DNA fragment as previously described (Shin et al., 2018). The presence of *Cre* was seen as an additional 554 bp DNA fragment (*Emx1* cre), and when a homozygous (glut3$^{flox/flox/Cre+}$) deletion (402 bp & 554 bp) occurred, this could be detected based on the presence of specifically sized DNA fragments observed upon genotyping of mouse lines.

2.2. Body and brain weight

Adult body weight was measured at 12 months of age in glut3$^{flox/flox/Emx1\text{-}Cre+}$ (KO) versus glut3$^{flox/flox}$ mice which served as controls. Following euthanasia, brains were retrieved after craniotomy and total brain weights were measured in KO and CON groups.

2.3. Blood glucose measurement

Following inhalational anesthesia with isoflurane, whole blood from 12-month-old mice was collected through puncture of the retro-orbital venous plexus and glucose concentrations were measured by the AlphaTRAK 2 glucometer (Zoetis, NJ).

2.4. Brain Studies in glut3$^{flox/fox/Emx1\text{-}Cre+}$ mice

2.4.1. Brain sample preparations

Mice were deeply anesthetized under inhalational isoflurane (4% for induction, and 1.25% to 1.5% for maintenance), and brains (2 month and 10–12 month old) collected after craniotomy performed after intraperitoneal administration of sodium pentobarbital (50–100 mg/kg). Brains were snap frozen in liquid nitrogen and stored at -80°C for subsequent Western blot analysis as previously described (Baldauf et al., 2020; Shin et al., 2018; Zhao et al., 2010). In other cases, mice were perfused with 4% paraformaldehyde in 0.1 M phosphate buffer, pH 7.4, and embedded in OCT compound for immunohistochemical analysis as previously reported by us (Baldauf et al., 2020; Ganguly et al., 2007; Shin et al., 2018; Zhao et al., 2010).

2.4.2. Brain protein concentrations by Western blot analysis

Brain homogenates were subjected to Western blots as previously described (Shin et al., 2018). The blotted membranes were sequentially incubated in primary antibodies consisting of the rabbit anti-GLUT3 (1/1000, from Takata, RRID:AB_2631293), synaptophysin (1/1000, Millipore, Cat# 04–1019, RRID:AB_1977519), β-tubulin (1/1000, Covance, Cat# MMS-435P, RRID:AB_2313773) and Map2 (1/1000, Neuromics, Cat# MO22116, RRID:AB_2737343) antibodies. The proteins were visualized using a Typhoon 9410 Phosphor imager (GE Healthcare Biosciences, Piscataway, NJ) by blotting with the enhanced chemiluminescence (ECL) plus detection kit (GE Healthcare BioSciences Corp., Piscataway, NJ) following horseradish peroxidase-labeled anti-IgG (for anti-mouse, 1/7000, Vector Cat# PI 2000, RRID:AB_2336177; for anti-rabbit, 1/5000, GE healthcare Cat# NA934, RRID:AB_772206) chosen based on the species in which primary antibodies (GE Healthcare Biosciences Corp., Piscataway, NJ) were raised. Each protein was quantified by using ImageQuant 5.2 software (GE Healthcare Biosciences, Piscataway, NJ) and normalized to vinculin (served as the internal loading control) as previously described (Baldauf et al., 2020; Shin et al., 2018).

2.4.3. Spatial localization by immunohistochemical studies

Sagittal brain sections (10 μm) and transverse placenta sections (10 μm) obtained by a cryostat (Leica RM2235; Leica Microsystems, Deerfield, IL) were subjected to immunofluorescence staining using rabbit anti-EMX1 (1/50, Thermo Fisher Scientific Cat# PA5-35373, RRID:AB_2552683) as the primary antibody, followed by corresponding secondary antibodies carrying the fluorescence tag of Alexa 488 (1/500, Jackson ImmunoResearch Labs Cat# 711–545-152, RRID:AB_2313584). DAPI was used for DNA staining, and sections subjected to microscopy as previously described (Shin et al., 2018).

2.4.4. Cortical pyramidal neuron patch clamp study

Coronal brain slices (300 μm) from the rostral (motor) or caudal (somatosensory) cerebral cortices (2–3 month and 10–12 month old male mice) were maintained in oxygenated artificial CSF. Cortical pyramidal neurons (CPNs) in layer V were recorded in voltage-clamp mode as described previously (Cummings et al., 2009). CPNs were identified by their typical triangular soma shape, the presence of a thick apical dendrite, and in some cases by addition of biocytin. First, basic membrane properties (cell capacitance, input resistance, and decay time constant) were determined using a depolarizing step voltage command (10 mV). The frequency of spontaneous glutamatergic (Vhold = −70 mV) and GABAergic (Vhold = +10 mV) synaptic currents was also estimated. After 3–5 min of baseline recording at −70 mV, the $GABA_A$ receptor antagonist bicuculline (10 μM) was applied in the bath and kept for 10 more min before washout. This treatment increases cortical excitability and can induce epileptiform activity manifested by large inward currents. Data were analyzed using Clampfit 10.3 software (Molecular Devices, Sunnyvale, California) and the number of paroxysmal events and their latency were determined. Spontaneous synaptic currents were analyzed using the Minianalysis program (Synaptosoft, version 6.0).

2.5. Neurobehavioral studies

Ten to 12-month-old adult mice were subjected to the rotarod, open field, contextual fear conditioning, Morris water maze, sociability and social novelty testing after habituation and adequate training as previously desscribed (Dai et al., 2017; Shin et al., 2018; Zhao et al., 2010).

2.5.1. Accelerating rotarod test

Evaluation of motor coordination and motor learning was achieved by performing the accelerating rotarod test (RotaRod3375-5, TSE system, Hamburg, Germany). The constant speed of 5 rpm was used at the first trial during the acquisition day. The rest of the four consecutive trials started at a beginning speed of 5 rpm but increased by 5 rpm after each 5 s up to a maximum speed of 60 rpm. Data were collected after the test subject mouse either demonstrated falling from the rod or stayed for 300 s at a maximum speed of 60 rpm.

2.5.2. Open field test

Assessment of anxiety, exploratory behavior and general locomotor activity was accomplished by placing each of the test mice individually in a square Plexiglas enclosure for 20 min. Their movements were recorded by video cameras and the different parameters measured which included total distance traveled in whole arena, percent of time spent in the center of the arena, average velocity and resting time, by the associated Topscan software (Clever Sys, Inc., Reston, VA).

2.5.3. Fear conditioning

For assessment of learning and memory about the associated environment with aversive experiences, contextual fear conditioning was performed. At acquisition trial, mice were placed in a chamber and received 0.75 mA electric foot shock 3 times within 5 min of contextual conditioning. Twenty-four hours after the training session, mice were returned to the same contextual environment and their freezing behavior was recorded with an associated video and software system in the absence of the associated shock (Med Associates Inc., Fairfax, VT).

2.5.4. Morris water maze test

The invisible platform test was performed to investigate spatial learning and memory in mice. Before the first trial, mice were initially trained to find the escaping platform (12 cm diameter) set in a constant place in a water maze pool (1 m diameter, water temperature = 24 °C), according to distal cues as achieved by placing the mice on the platform for 30 s. They were returned to the platform if they jumped off 3 times and were subsequently placed in the pool to swim for 30 s. First training trial began after a 2 min interval. Each mouse was released in the pool from different starting quadrants that did not contain the platform. They were allowed to swim until they found the platform or when 60s had elapsed. Subsequently they were allowed to stay on the platform or placed on the platform for 5 s. Three trials were performed per day and these trials lasted for 5 days. The latency to find the platform was recorded for each trial. To monitor whether the mice had learned the platform location accurately or found the platform by chance, they were given a single platform trial after completion of the training trials by removing the platform and allowing them to swim for 60 s in the pool from the same beginning location for each mouse. Finally, they were given 2 consecutive visible platform trials (made visible by locating a visible cue on the platform). Tracking information was processed by the Topscan software.

2.5.5. Social interaction

An interconnected three-chambered box was used for evaluation of memory of interaction in subject mice. Test included three phases: habituation (phase I), assessment of sociability (phase II) and social recognition (phase III) phases. At the habituation phase, the subject mouse was placed in the middle chamber and allowed to explore all chambers for 10 min. In phase II, after habituation of the subject mice for 10 min one day before testing, a novel mouse (sex-matched with subject mouse) was placed inside an upside-down wire cup in either the left or right chamber, and the other side contained an empty wire cup. The subject mouse was then returned to the middle chamber. Exploration activity and time spent with either the empty cup or the cup with novel mouse were recorded and scored by the Topscan software. In phase III a new and unfamiliar mouse was placed in the empty wire cup while the opposite side chamber of the apparatus contained the familiar mouse from phase II. Time spent within 10 min with the novel mouse versus the familiar mouse was compared.

2.6. Statistical analyses

All data are shown as mean ± SEM. Student's *t*-test or Fisher's exact test was used when two groups were compared simultaneously. Student's t-test with Bonferroni's correction when indicated for multiple parameters being tested simultaneously or when indicated one-way analysis of variance (ANOVA) was used for more than two groups being compared simultaneously. When significant differences were identified, this was followed by the Fisher's PLSD post-hoc analysis to determine inter-group differences. Null hypothesis was rejected at a $p < 0.05$. All Statistical analyses were performed using a GraphPad Prism 7 software program (RRID:SCR_002798).

3. Results

Our results depict only males when no differences emanated between the sexes, while both sexes are shown separately when sex-specific differences were detected.

3.1. Confirmation of EMX1 expression in brain and placenta

The purpose of examining EMX1 expression in placenta and brain was to distinguish between the placental versus the brain effects that underlie the ultimate phenotypic changes emanating in the Emx1-glut3 KO mice. Therefore, we initially examined the presence of EMX1 protein in adult female brain and gestation 19 placentas. EMX1 demonstrated a nuclear distribution mimicking that seen with DAPI within the brain cortex (Fig. 1A), but not in cerebellum and hypothalamus (Supplementary Fig. S1). In contrast to the brain cortex, no EMX1 expression was noted in the late gestation placenta (Fig. 1B). This finding suggests that placental *glut3* gene in the Emx1-glut3 KO mice will not be deleted and therefore only brain cortical *glut3* gene deletion will be encountered and underlie the emerging phenotype.

3.2. Assessment of body weight, brain weight and blood glucose concentrations

We next examined the effect of brain glut3 gene deletion upon body and brain weights and circulating plasma glucose. Adult body and brain weights demonstrated sex-specific differences, while male body weights were no different in the Emx1-glut3 KO versus the floxed glut3 control mice (Fig. 2A), brain weights were observed to be lower (Fig. 2B). In contrast, female body weights were lower (Fig. 2D) while no difference in brain weights emerged (Fig. 2E). We next depicted brain weights as a ratio to body weights and noted no difference in males (KO = 0.011 ± 0.00041 versus CON = 0.011 ± 0.00047; df = 22, t-statistic = 0.063, *p*-value = 0.95; $n = 12$ in each group), while a relative increase in female brain to body weights ratio emerged (KO = 0.013 ± 0.00059 versus CON = 0.011 ± 0.00061; df = 18, t-statistic = 2.148, p-value = 0.05; $n = 10$ in each group). In both sexes no differences in blood glucose were seen, although trends towards an increase in males (Fig. 2C) and a decrease in females was seen (Fig. 2F).

3.3. Expression of GLUT3 protein, Synaptophysin and β-III tubulin

To confirm glut3 gene deletion, brain region specific quantification of the GLUT3 protein was undertaken. Region-specific quantification of the GLUT3 protein in the adult brain (males and females) revealed no change in the glut3 KO 2 month mice particularly in the hypothalamus and cerebellum, however a decrease was seen in the cortex and brain stem. Quantification of the cortical GLUT3 revealed a ~ 50% decrease (Fig. 3A), since Emx1 induced transcription/translation would occur only in the excitatory neurons. Further quantification of synaptophysin (an axonal marker; Fig. 3B) and β-III tubulin (neuronal marker; Fig. 3C) revealed no statistically significant differences between glut3 KO and floxed controls within the cortical regions. Assessment of cortical GLUT3 protein concentrations at a later age of 10–12 months also revealed the persistence of a 67% decrease in glut3 KO versus the age-matched floxed controls (Fig. 3D).

3.4. Cortical patch-clamp study

We next examined the functional effect of reduced GLUT3 limited to Emx1 expressing neurons on cortical pyramidal neuron basic membrane properties, spontaneous synaptic activity, and functional seizure susceptibility. Patch clamp studies in 2–3 month old mice revealed no significant differences in cell membrane capacitance (247 ± 15 pF in *glut3* KO and 246 ± 16 pF in CON, $n = 13$ and 12 cells respectively, $p = 0.96$; input resistance 80.8 ± 6 MΩ in *glut3* KO and 81.3 ± 10 MΩ in CON, $p = 0.97$; decay time constant 4.1 ± 0.3 in *glut3* KO and 4.1 ± 0.4 in CON, $p = 0.92$). Similarly, no significant differences in the frequency of spontaneous glutamatergic (6.6 ± 1.2 Hz in *glut3* KO and 5.8 ± 1.5 Hz in CON, $p = 0.67$) and GABAergic (14.7 ± 1.7 Hz in *glut3* KO and 12.5 ± 2.2 Hz in CON, $p = 0.43$) synaptic events in *glut3* KO compared to CON cells were observed. The effects of $GABA_A$ receptor blockade with bicuculline were tested in CPNs from CON ($n = 11$) and *glut3* KO mice (n = 11). Significant differences in functional seizure susceptibility, assessed by the occurrence of paroxysmal discharges in slices, began to emerge. All CPNs from *glut3* KO mice displayed paroxysmal activity (11/11, 100%), whereas only 7/11 (63.6%) displayed paroxysmal discharges in CON animals ($p = 0.027$, Chi-square test) (Fig. 4A,C). In addition, the frequency of paroxysmal discharges was signifcantly greater and the latency to the first discharge was shorter in CPNs from *glut3* KO compared with CON mice (Fig. 4B,D). Similar differences were forthcoming in the 10–12 month old glut3 KO versus age-matched CON mice as well (not shown). These findings indicate that cortical pyramidal neurons lacking GLUT3 are hyperexcitable.

3.5. Neurobehavioral tests

To assess the impact of earlier changes in cortical GLUT3 concentrations and patch clamp recordings on the subsequent phenotype of *glut3* KO adult mice, neurobehavioral responses were next assessed employing various testing modalities in 10–12 month old mice. The accelerating rotarod test failed to reveal statistically significant differences in motor performance between the two genotypes, although the female glut3 KO mice displayed a much shorter latency to fall when compared to controls (Fig. 5A,E). Open field testing revealed no differences in velocity or the resting times, however in both males and females, the total path length covered was increased in glut3 KO versus the controls (Fig. 5B,F). However, the time spent in exploration within the center of the field was reduced (Fig. 5C,G) in both sexes in the glut3 KO versus the controls. Upon subjecting the mice to contextual fear conditioning, a reduction in time spent freezing was evident in glut3 KO compared to controls (Fig. 5D,H), achieving statistical significance in the females (Fig. 5H). Spatial memory and cognition were assessed by the Morris water maze test, where no difference in speed was observed. However the female more than the male glut3 KO mice versus sex-matched controls spent less time in the target quadrant, while spending more time in other quadrants (left quadrant in males, and

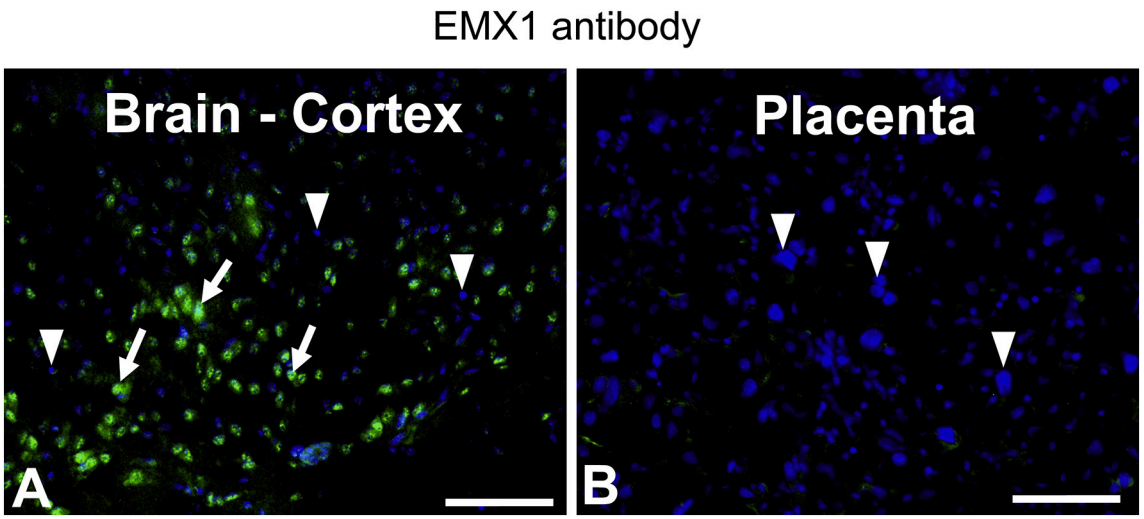

Fig. 1. Immunofluorescence localization of EMX1 in the brain cortex of 2-month-old CON mice and in E19 placenta. Arrows: EMX1 Alexa 488 positive nuclei (green); Arrowheads: EMX1 Alexa 488 negative nuclei, stained with DAPI (blue). A. Brain cortex; B. Placenta. Scale bar = 100 μM.

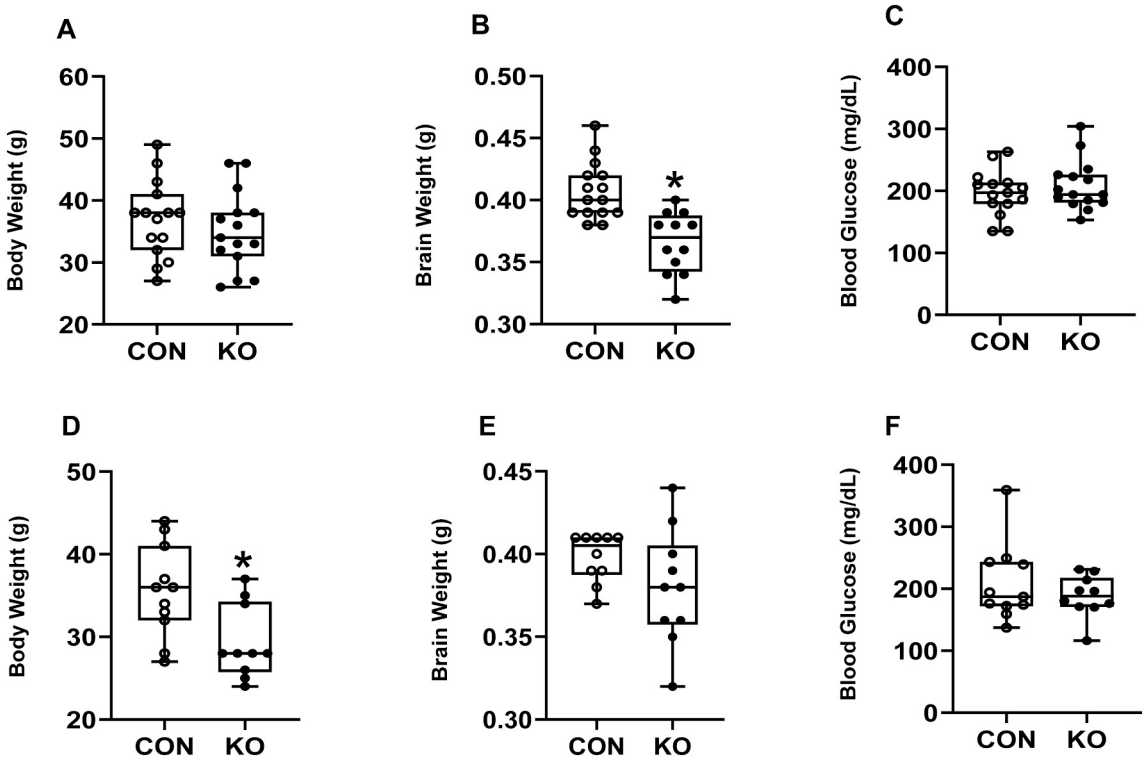

Fig. 2. Body weight, brain weight and blood glucose at the basal state in the male (A-C) and female (D–F) 12-month-old mice. Unpaired *t*-test determined significant differences between CON and KO mice. A, Body weight, t statistic [df: 28] = 0.8179, *p*-value = 0.4203, *n* = 15 each for CON and KO; B, Brain weight, t statistic [df: 25] = 4.498, *p-value = 0.0001, n = 15 for CON and *n* = 12 for KO; C, Blood glucose level, t statistic [df: 28] = 0.8579, p-value = 0.3982, n = 15 each for CON and KO. D, Body weight, t statistic [df: 19] = 2.818, **p*-value = 0.0110, *n* = 11 for CON and *n* = 10 for KO; E, Brain weight, t statistic [df: 18] = 1.500, p-value = 0.1510, n = 10 each for CON and KO; F, Blood glucose level, t statistic [df: 19] = 0.9147, *p*-value = 0.3718, n = 11 for CON and *n* = 10 for KO.

opposite quadrant in females) (Fig. 6A,D). While testing sociability, both the male and female glut3 KO mice trended towards spending more time with the mouse rather than the empty cup, with females achieving statistical significance (Fig. 6B,E) when compared to controls. In social novelty recognition test, again only female glut3 KO mice spent more time with the unfamiliar versus familiar mouse, while the male counterpart did not display this difference (Fig. 6C,F).

4. Discussion

In our present study, we successfully created an adult phenotype that lacked GLUT3 in specific neurons localized to the cortex. Despite a reduction of GLUT3 observed in the brain stem, no impact on physiological functions such as breathing (respirations) was observed. Such survival into adult life was successful given that EMX-1 is not expressed in the placenta but mainly in the cerebral cortex. While reducing GLUT3 in these brain anatomical locations, no disruption of synaptophysin (axonal marker) or tubulin (neuronal marker) expression in the adult cortex was observed, although lower trends were noticed. However, a reduction in male brain weights emerged with no such change in the female counterpart. More globally, no changes in circulating glucose were seen, and while whole body weights did not change in males, a reduction was evident in females. The reason for this sex-specific difference is unknown and needs further investigation.

Examination of seizure susceptibility in electrophysiological patch clamp experiments demonstrated earlier occurrence and increased frequency of paroxysmal discharges upon bicuculline $GABA_A$ receptor antagonism. This suggests that lack of GLUT3 limited in Emx-1 expressing neurons alone exaggerates the excitatory phenotype even during adult life. Neurobehavioral testing revealed that the lack of GLUT3 in excitatory neurons led to a hyperactive and anxious phenotype with deficiencies in contextual and spatial memory supporting cognitive difficulties. In contrast, sociability testing revealed excessive socialization with an unfamiliar mouse perhaps related to impulsivity. Most striking was the fact that while both males and females demonstrated similar trends in various neurobehavioral tests, most often the female glut3 KO revealed statistical differences. This was most evident in social novelty recognition testing. This may relate to male mice demonstrating considerable inter-mouse variability compared to females, or due to other physiological reasons. In the human, both males and females develop ADHD although the presenting symptomatology as an adult may differ. In males most of the symptoms are externalized with evidence of disruptive behaviors, while in the case of females they are internalized such as inattentiveness and anxiety (Stibbe et al., 2020). In our present study, an adult with glut3 gene loss-of-function mutation in excitatory glutamate neurons revealed distinct features reminiscent of the ADHD described previously in human studies along with glut3 polymorphisms (Merker et al., 2017). In this study both males and females were enrolled but features were not differentiated between the two sexes (Merker et al., 2017). In addition, these polymorphisms in some cases revealed gain-of-function when assessed by GLUT3 mRNA concentrations in peripheral circulating mononuclear cells which could not be replicated when corresponding protein concentrations were assessed (Jansch et al., 2018). Thus it is still not clear if the previously reported increased incidence (doubling) of these GLUT3 polymorphisms result in gain-of-function as presented, or loss of function, or no GLUT3 protein mediated functional change (Merker et al., 2017; Ziegler et al., 2020).

When a comparison is made of our present findings to that previously reported by us (Shin et al., 2018) where a CaMK2 related glut3 mutation was examined in adult mice, while there are similarities, distinct differences also emerge. In contrast to our present Emx-1-glut3 null mice that only affected the glutamate expressing neurons, CaMK2-glut3 null mice failed to demonstrate any phenotypic changes at 2–3 months of

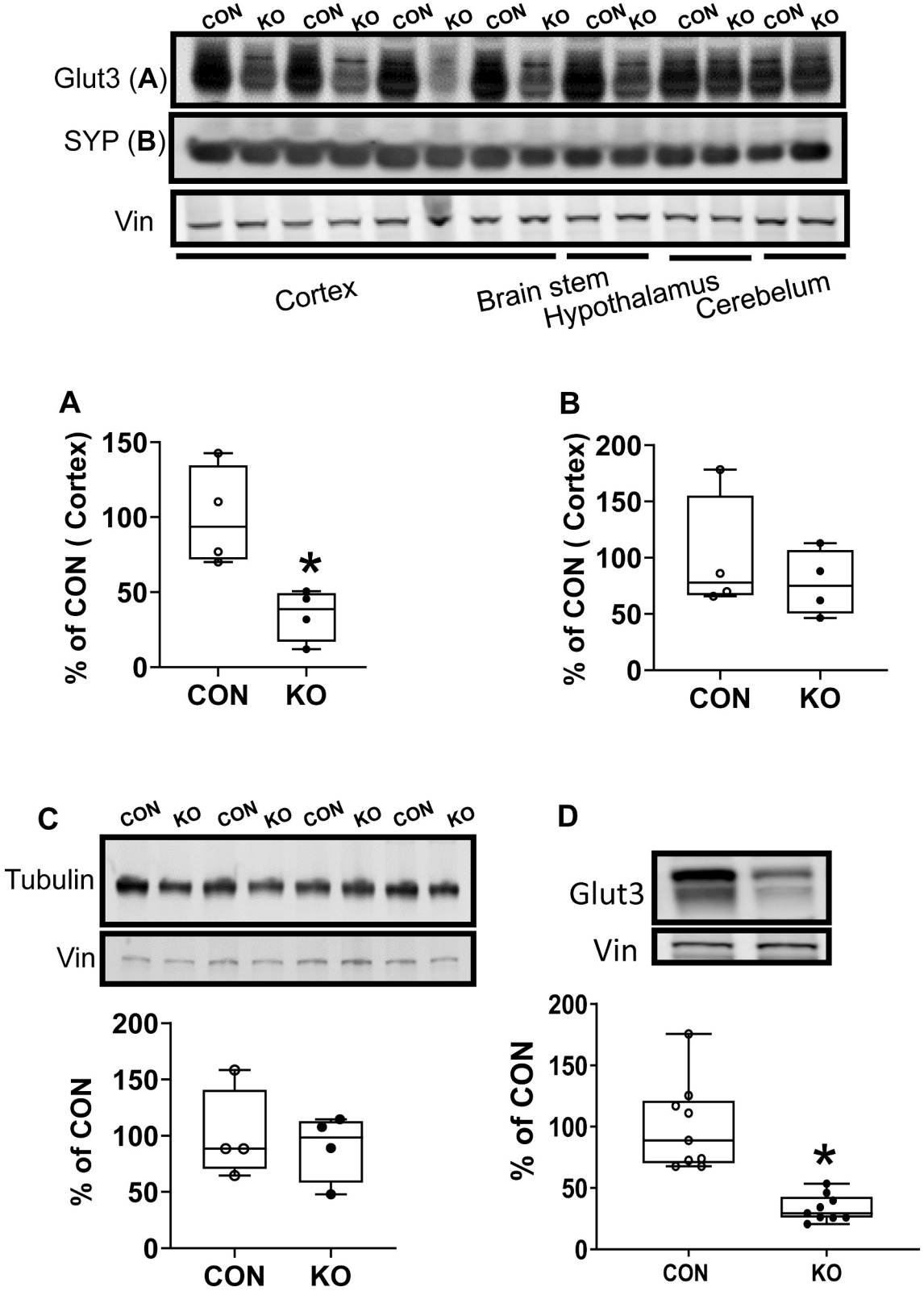

Fig. 3. Western blot analysis of Glut3 (A and D), Synaptophysin (SYP)(B) and Tubulin (C) proteins in the cerebral cortex of 2 month (A-C) or 10-12-month-old mice (D). Top, Representative Western blots with Glut3, Synaptophysin (SYP) and Tubulin shown above and vinculin (internal control) shown below. Bottom, Densitometric quantification of corresponding proteins shown as percent of CON. A, the expression of GLUT3 was reduced significantly in KO by 60% compared to CON. (t statistic [df: 6] = 3.451, **p*-value = 0.0136 $n = 4$ each for CON and KO, by unpaired *t*-test). B, there was no difference between CON and KO mice with SYP (t statistic [df: 6] = 0.7476, p-value = 0.4830), n = 4 for each group. C, there was no difference between CON and KO mice in the case of Tubulin (t statistic [df: 6] = 0.4021, p-value = 0.7015), n = 4 for each group. D, the expression of GLUT3 was reduced significantly in KO by 67% compared to CON. (t statistic [df: 16] = 5.297, **p*-value <0.0001, $n = 9$ each for CON and KO, by unpaired *t*-test).

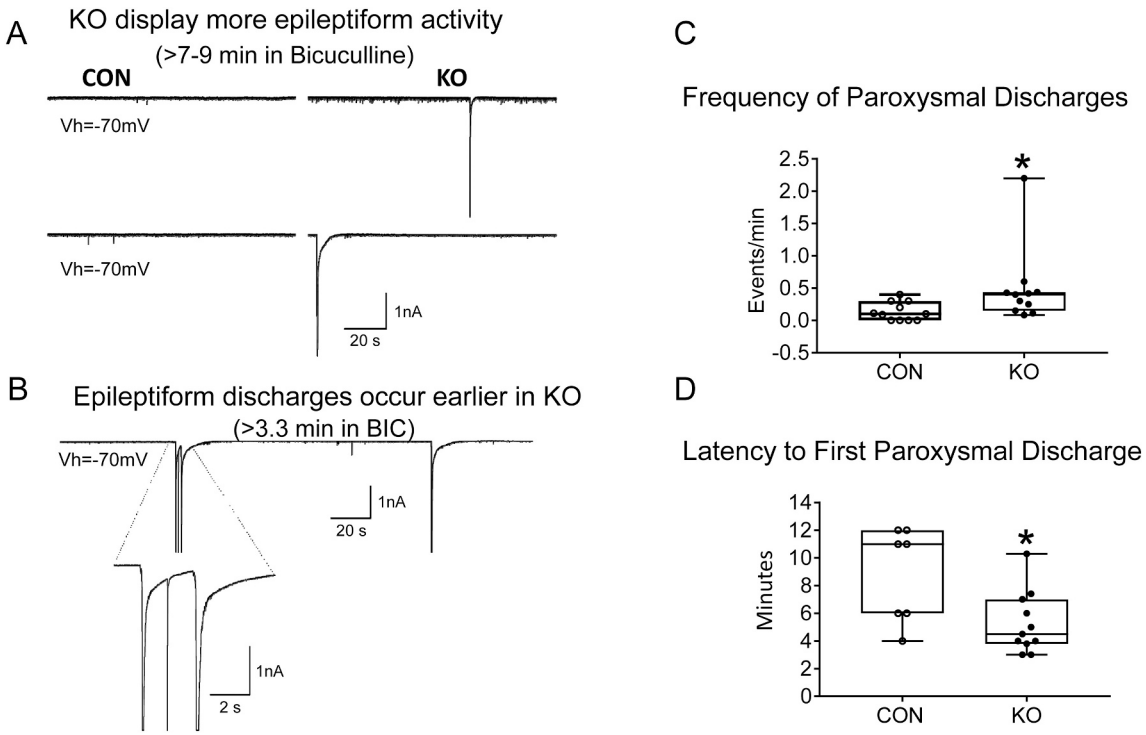

Fig. 4. A. Traces correspond to patch clamp recordings (voltage clamp mode) from 2 to 3 month old 6 CON (glut3$^{flox/flox/Emx1\text{-}Cre-}$) and 4 KO (glut3$^{flox/flox/Emx1\text{-}Cre+}$) mice and their cortical pyramidal neurons (CPNs) after 7–9 min of $GABA_A$ receptor antagonist bicuculline (10 μM) application. While all CPNs from KO mice displayed paroxysmal discharges, 4 out of 11 cells from CON mice did not generate discharges and the remainder displayed discharges after long latencies. In addition, discharges from KO mice were more complex (e.g., "doublets") (see B panel). (CON, n = 11 cells from 6 mice; KO, n = 11 cells from 4 mice). Total paroxysmal events: CON = 15, KO = 54. B. While paroxysmal discharges only exceptionally occurred before 7–9 min in CON cells, many KO cells showed paroxysmal activity within the first 5 min after bicuculline (GABA inhibitor) application. Notice also that this cell displayed a complex discharge ("doublet" discharge plus action potential in between) just 3.3 min after bicuculline. C. Events/min of paroxysmal discharges were increased in KO mice when compared to CON mice, *$p = 0.01$. D. Mean latency to the first paroxysmal discharge was significantly decreased in CPNs from the KO group when compared to the CON group ($p = 0.015$, 7 CON and 11 KO).

age. Most of the features only emerged at 8–10 months of age (Chen et al., 2001; Shin et al., 2018). Thus, unlike the Emx1-glut3 null mice, CaMK2-glut3 while also targeting more globally all excitatory pyramidal neurons, is expressed phenotypically more so in the aging mice rather than in the young adult mice. This may be because Emx-1 plays a role during early cortical patterning and development (Stocker and O'Leary, 2016), unlike CaMK2 which is a signaling molecule developing subsequently after accruing some life-time experiences and neuronal stimulation (Lisman et al., 2012; Zalcman et al., 2018). Further, CaMK2 is involved in long term potentiation (LTP) (Lisman et al., 2012). Differences in epileptiform activity also emerged. No changes were evident at 2 months of age in the CaMK2-glut3 null mice, only appearing later at 10 months of age. Most importantly, rather than changes in sEPSCs frequency, a reduction in sIPSCs was evident (Shin et al., 2018). In contrast, Emx1-glut3 null mice revealed increased excitatory activity as early as at 2–3 months of age, culminating in earlier occurrence and increased frequency of epileptiform activity, which was exaggerated in the presence of a $GABA_A$ antagonist. Thus it appears that Emx-1-glut3 null phenotypic changes emerged earlier in the young adult, while CaMK2-glut3 null phenotypic changes emerge much later at the beginning of aging.

Neurobehavioral testing revealed in CaMK2-glut3 null mice (Shin et al., 2018), more time spent in the center, while in the Emx1-glut3 null mice less time was spent in the center than periphery in Open Field tests. This supports a lack of fear for exploration of the unknown in CaMK2-glut3 mice, but anxiety in the Emx1-glut3 null mice who seem to take cover in the darker peripheral regions. However, while the Emx1-glut3 null mice covered much more total path length, no such change was seen with the CaMK2-glut3 null mice, attesting to hyperactivity in the former. Fear conditioning revealed a difference as well. In the Emx1-glut3 null mice, less time was spent in a frozen state, while in the CaMK2-glut3 null mice, more time was spent freezing versus their respective age and sex matched controls. This divergence supports a longer time habituating to a fear response or a lack of fear in the CaMK2-glut3 null mice, while Emx-1-glut3 null mice reveal a lack of contextual memory to fear conditioning along with a hyperactive state. In both cases, spatial memory and cognition were deficient, as less time was spent in the target quadrant in a Morris Water maze test. Testing for sociability and recognition of novelty again revealed more time spent with the unfamiliar mouse attesting to lack of fear of novelty or impulsivity as the case may be. The CaMK2-glut3 null mice also revealed motor deficits in the rotarod test, akin to the shorter latency to fall particularly evident in the female Emx1-glut3 mice. However, previously in classical glut3 heterozygotes, no motor deficit was evident in the rotarod test (Zhao et al., 2010). These similarities with certain distinct features may relate to age-differences at when the lack of GLUT3 is expressed. To overcome this, we age-matched the Emx-1-glut3 null mice to that performed previously with CaMK2-glut3 null mice (Shin et al., 2018) by undertaking neurobehavioral testing in older mice in the present study. However, sex-specific differences cannot be ruled out entirely, as the CaMK2-glut3 mice studied were male (Shin et al., 2018) and the Emx-1-glut3 mice comprised of both sexes. Differences between the two null mice may also be related to connectivity differences. While EMX1 and CaMK2 are found in pyramidal excitatory neurons of the somatosensory cortex and hippocampus (Achterberg et al., 2014; Chan et al., 2001; Gorski et al., 2002), differing outputs based on synaptic connections may be responsible for establishing distinct neural circuitry and neurobehaviors. In addition, CaMK2 related GLUT3 loss was more global as also seen in the

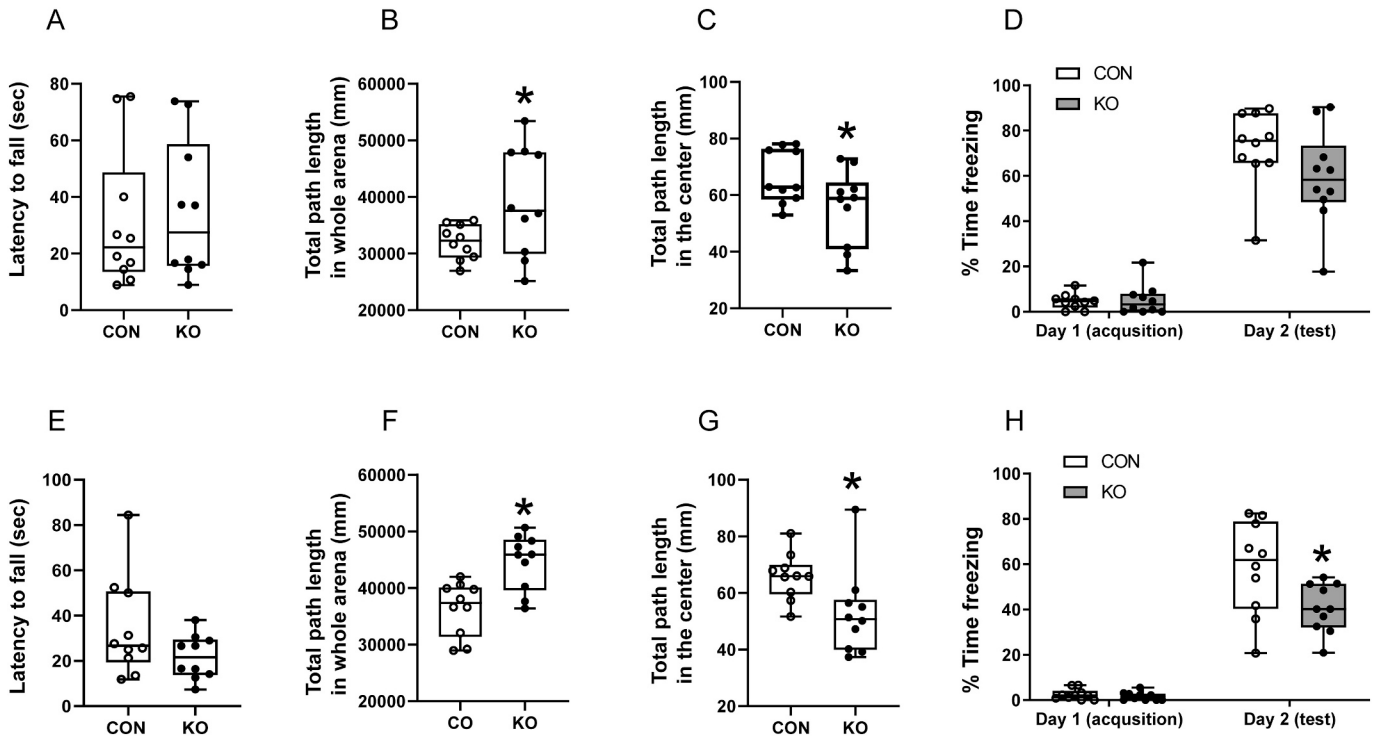

Fig. 5. Rotarod, open-field task and fear conditioning tests in male (A-D) and female (*E*-H) at 10 to 12-month-old mice. A, Accelerating rotarod test was performed in male (A) and female (E). In male, there was no difference in the latency to fall between KO and CON mice (A), unpaired *t*-test, t statistic [df: 18] =0.3326, *p*-value = 0.7433, $n = 10$ each for CON and KO mice. In female, KO mice showed a decline supporting a sooner fall from the rod than CON mice (E), unpaired *t*-test, t statistic [df: 18] =1.638, p-value = 0.1188, n = 10 each for CON and KO mice. B–C & F-G, Open-field tasks were performed and the total path length within the whole arena (B & F) and distance traveled in center of the arena (C & G) are shown. Distance traveled in the whole arena (B & F) reflected the KO mice covering greater total path length of the whole arena compared to CON by both male (B) and female (F). In male, unpaired *t*-test with Welch's correction, t statistic [df: 17.98] =3.813, *p-value = 0.0013, $n = 10$ each for CON and KO mice; In female, unpaired *t*-test with Welch's correction, t statistic [df: 10.83] =2.261, *p-value = 0.0454, n = 10 each for CON and KO mice. Distance traveled in the center of arena (C & G), while male KO mice covered less distance in the center compared to CON mice, no significant difference was noted (C), unpaired *t*-test with Welch's correction, t statistic [df: 16.20] = 2.091, p-value = 0.0526, $n = 10$ for both CON and KO mice. Female KO mice traveled less distance in the center of the arena and demonstrated tendencies in staying near the corners (G), unpaired *t*-test with Welch's correction, t statistic [df: 13.87] = 2.399, *p-value = 0.0311, $n = 10$ for both CON and KO mice. D & H, Contextual fear conditioning, Although male KO mice showed a similar impaired fear conditioning pattern with no significant difference (D), two-way ANOVA followed by Sidak's multiple-comparisons test.: interaction, F statistic [df:1,36] = 2.436, $p = 0.1273$; day1 to day 2, F statistic [df: 1, 36] = 187.4, $p < 0.0001$; genotype, F statistic [df:1, 36] = 2.01, $p = 0.1648$. p-value for day 2 = 0.0827, $n = 10$ for both CON and KO), female KO mice showed impaired contextual fear conditioning. KO mice spent significantly less time freezing compared to CON (H), two-way ANOVA followed by Sidak's multiple-comparisons test.: interaction, F statistic [df:1,36] = 5.271, $p = 0.0276$; day1 to day 2, F statistic [df: 1, 36] = 164.1, $p < 0.0001$; genotype, F statistic [df:1, 36] = 6.33, $p = 0.0165$. *p-value for day 2 = 0.0033, n = 10 for both CON and KO.

amygdala (limbic system), striatal GABA interneurons and cerebellar Purkinje cells (Shin et al., 2018), which was not the case in Emx1-glut3 null mice.

Most importantly, Emx1 dependent glut3 expression may have disrupted early life patterning of the developing brain resulting in alterations of synaptic connectivity, the effect of which presents in the adult. This early life effect may mimic cognitive programming. In contrast, CaMK2-related GLUT3 absence may be a feature gained only during adulthood lacking the component of early life impact on neurodevelopment. This may explain the differences that emerge in the adult lacking neuronal glut3. Further, the Emx1-glut3 KO mice revealed neurobehavioral changes more so in females than males consistent with a hyperactivity/anxiety/impulsivity phenotype, while both sexes were equally affected by cognitive deficiencies.

Our studies differentiating phenotypes between loss of cortical GLUT3 early in life impacting the adult phenotype (as in the Emx1-glut3 KO) versus that which emerges much later in life (CaMK2-glut3 KO) has far reaching implications for human neurodevelopmental and psychiatric disorders. Neurobehavioral phenotypic presentations vary depending on whether the clinical symptoms are in response to neurodevelopmental or neurodegenerative disorders. AHDH/Anxiety disorders that emerge as early as in childhood are due to aberrations in neurodevelopment (Merikangas and Almasy, 2020). The key diagnostic differentiator in children between autism spectrum disorders (ASDs) and ADHD is deficits in inhibitory control in the latter, while both present with cognitive deficits, particularly in executive functioning (Stibbs et al). ADHD is often a co-morbidity of ASDs, and considered a cognitive endophenotype of such a presentation. In fact, ASDs also encompass anxiety as a clinical symptom with deficits in sociability with stereotypical behaviors (Sharma et al., 2018).

Our previous studies in the classical heterozygous glut3 KO mice revealed changes in neurobehaviors that mimicked ASDs in children (Zhao et al., 2010). This presentation was in response to a reduction in GLUT3 in all neurons, while our current Emx1-glut3 KO is a complete loss of GLUT3 in excitatory neurons alone. In the former, neurobehavioral deficits emerged early (7d postnatal age to 2 months), while in the latter we noted changes in patch-clamp studies as early as 2–3 months of age. Thus, the dose and extent of neuronal involvement dictates the emergence of clinical symptomatology, ranging from ADHD/Anxiety disorder to ASDs. Ultimately, both being neurodevelopmental disorders that require an even earlier age investigation in the future. Changes in neurodevelopment have the propensity of permanently altering neurobehavioral outcomes into adult life. Such an effect constitutes developmental programming of neurobehavior with far reaching consequences (Merikangas and Almasy, 2020).

In conclusion, selective lack of glut3 in EMX1 expressing glutamate

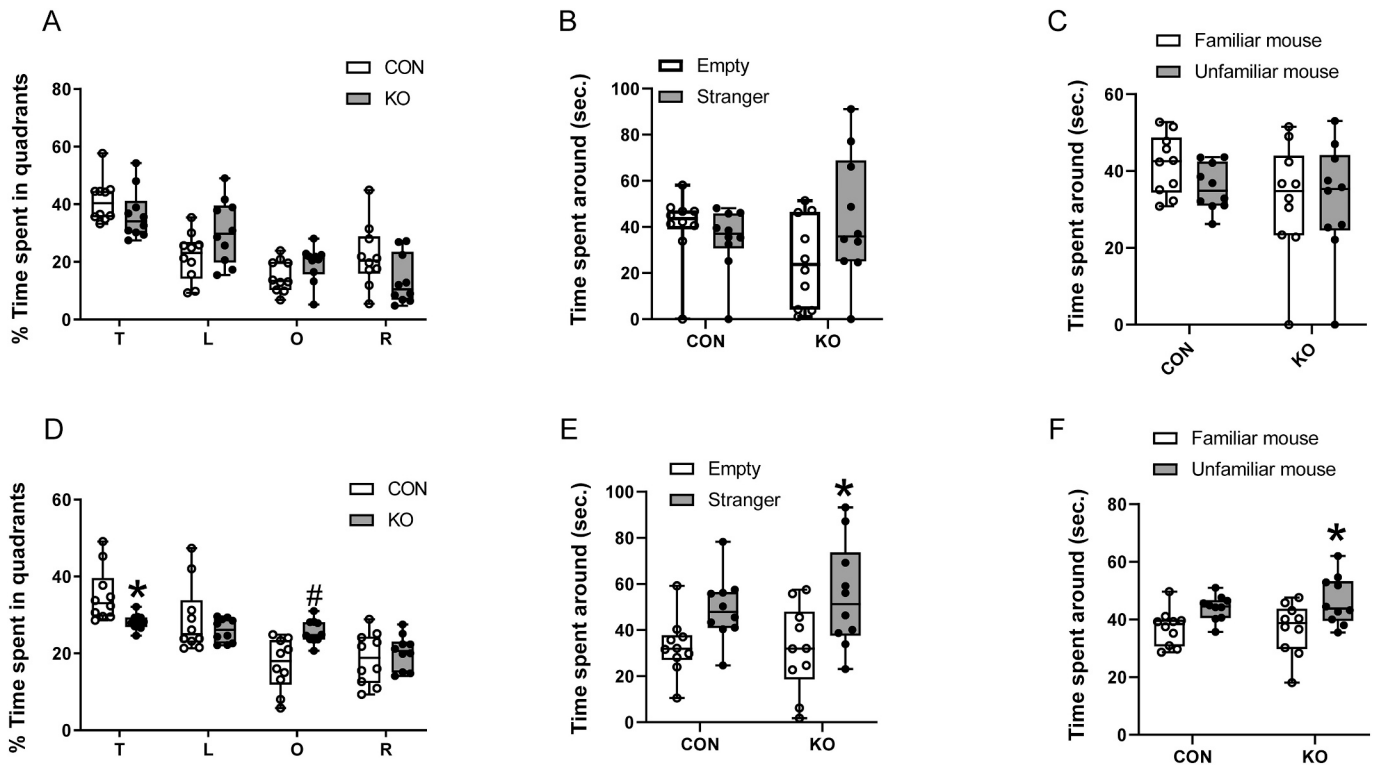

Fig. 6. Water maze and social interaction tests were performed in male (A-C) and female (D–F) 10 to 12-month-old mice. A & D, Time spent in each quadrant (T, target quadrant; L, left quadrant; O, opposite quadrant; R, right quadrant) was measured in the probe trial in which the platform was removed from the pool. In male (A), glut3 KO mice spent less time in target quadrant than CON although no significant difference was detected. glut3 KO mice spent more time in opposite quadrant that did not achieve statistical significance, two-way ANOVA followed by Sidak's multiple-comparison test; interaction, F statistic [df: 3, 72] = 4.216, $p = 0.0084$; Time spent, F statistic [df:3,72] = 27.58, $p < 0.0001$; genotype, F statistic [df:1, 72] = 1.696e-006, $p = 0.9990$. $p = 0.6190$ for target quadrant; $p = 0.0951$ for left quadrant; $p = 0.7209$ for opposite quadrant; $p = 0.1345$ for right quadrant. Female (D), glut3 KO mice spent significantly less time in target quadrant than CON, with more time spent in the opposite quadrant, two-way ANOVA followed by Sidak's multiple-comparisons test; interaction, F statistic [df: 3, 72] = 6.662, $p = 0.0005$; Time spent around, F statistic [df:3,72] = 19.18, $p < 0.0001$; genotype, F statistic [df:1, 72] = 0.0009763, $p = 0.9752$. *$p = 0.0342$ for target quadrant; $p = 0.6887$ for left quadrant; #$p = 0.0056$ for opposite quadrant; $p = 0.9606$ for right quadrant. B & E. Sociability test in male (B) and female (E) mice revealed that while both male and female KO mice spent more time compared to respective CON with the novel mouse than with the empty wire cup, only females achieved statistical significance. In male, two-way ANOVA followed by Sidak's multiple comparison test: interaction, F statistic [df: 1, 36] = 3.835, $p = 0.0580$; time spent around, F statistic [df: 1, 36] = 0.0002, $p = 0.6270$; genotype, F statistic [df: 1, 36] = 8.912, $p = 0.2999$; n = 10 for both CON and KO. In KO, Empty vs Stranger $p = 0.2183$; in female, two-way ANOVA followed by Sidak's multiple comparison test: interaction, F statistic [df: 1, 36] = 0.3211, $p = 0.5744$; time spent around, F statistic [df: 1, 36] = 0.1624, $p = 0.6893$; genotype, F statistic [df: 1, 36] = 12.47, $p = 0.0012$; n = 10 for both CON and KO *$p = 0.0376$. C & F. Social novelty test conducted in male (C) and female (F) mice, the male glut3 KO mice were no different from CON in time spent with novel mouse or familiar mouse (C), two-way ANOVA followed by Sidak's's multiple comparison test; interaction, F statistic [df:1,36] = 0.6379, $p = 0.4297$; Time spent around, F statistic [df: 1, 36] = 2.849, $p = 0.1001$: genotype, F statistic [df: 1, 6] = 0.6818, $p = 0.4144$; n = 10 for both CON and KO. Female glut3 KO mice spent significantly more time with the novel mouse rather than the familiar mouse (F) (unfamiliar versus familiar of CON, $p = 0.2092$), two-way ANOVA followed by Sidak's's multiple comparison test; interaction, F statistic[df:1,36] = 0.3729, $p = 0.5453$; Time spent around, F statistic [df: 1, 36] = 0.2178, $p = 0.6435$: genotype, F statistic [df: 1, 36] = 13.33, $p = 0.0008$; n = 10 for both CON and KO. Unfamiliar versus familiar in the case of glut3 KO, *$p = 0.0279$.

excitatory pyramidal telencephalic neurons revealed phenotypic changes in the young adult that were consistent with cortical pyramidal neuron hyperexcitability, continuing into older ages seen as anxiety with lack of fear for novelty and a tendency towards hyperactivity and impulsivity. In addition, deficiencies in contextual and spatial memory and cognition emerged. Unlike the much later chronological emergence of the phenotype resulting from a lack of glut3 in CaMK2 expressing excitatory pyramidal somatosensory, amygdaloid and cerebellar Purkinje cells (Shin et al., 2018), similarities in neurobehavioral elements occurred with distinction related to epileptiform activity and contextual fear conditioning. Our present characterization of the phenotype in the young and older adult carrying a neuronal glut3 mutation allows for testing the association described in a subset of older adult patients with ADHD and glut3 loss-of-function gene mutations.

Supplementary data to this article can be found online at https://doi.org/10.1016/j.expneurol.2021.113603.

Declaration of Competing Interest

The authors declare no conflict of interest.

Acknowledgements

This work was supported by grants from National Institute of Health, United States of America: HD08106 and HD41230 (to S.U.D.). We thank Monique Awanyai, Joshua Gilardi, Mi Lim Chung for assistance with mouse genotyping.

References

Achterberg, K.G., Buitendijk, G.H., Kool, M.J., Goorden, S.M., Post, L., Slump, D.E., Silva, A.J., van Woerden, G.M., Kushner, S.A., Elgersma, Y., 2014. Temporal and region-specific requirements of alphaCaMKII in spatial and contextual learning. J. Neurosci. 34, 11180–11187.

Baldauf, C., Sondhi, M., Shin, B.C., Ko, Y.E., Ye, X., Lee, K.W., Devaskar, S.U., 2020. Murine maternal dietary restriction affects neural Humanin expression and cellular profile. J. Neurosci. Res. 98, 902–920.

Carayannopoulos, M.O., Xiong, F., Jensen, P., Rios-Galdamez, Y., Huang, H., Lin, S., Devaskar, S.U., 2014. GLUT3 gene expression is critical for embryonic growth, brain development and survival. Mol. Genet. Metab. 111, 477–483.
Chan, C.H., Godinho, L.N., Thomaidou, D., Tan, S.S., Gulisano, M., Parnavelas, J.G., 2001. Emx1 is a marker for pyramidal neurons of the cerebral cortex. Cereb. Cortex 11, 1191–1198.
Chen, R.Z., Akbarian, S., Tudor, M., Jaenisch, R., 2001. Deficiency of methyl-CpG binding protein-2 in CNS neurons results in a Rett-like phenotype in mice. Nat. Genet. 27, 327–331.
Connealy, B.D., Northrup, H., Au, K.S., 2014. Genetic variations in the GLUT3 gene associated with myelomeningocele. Am. J. Obstet. Gynecol. 211 (305), e301–e308.
Cummings, D.M., Andre, V.M., Uzgil, B.O., Gee, S.M., Fisher, Y.E., Cepeda, C., Levine, M. S., 2009. Alterations in cortical excitation and inhibition in genetic mouse models of Huntington's disease. J. Neurosci. 29, 10371–10386.
Dai, Y., Zhao, Y., Tomi, M., Shin, B.C., Thamotharan, S., Mazarati, A., Sankar, R., Wang, E.A., Cepeda, C., Levine, M.S., Zhang, J., Frew, A., Alger, J.R., Clark, P., Sondhi, M., Kositamongkol, S., Leibovitch, L., Devaskar, S.U., 2017. Sex-specific life course changes in the neuro-metabolic phenotype of Glut3 null heterozygous mice: ketogenic diet ameliorates electroencephalographic seizures and improves sociability. Endocrinology. 158, 936–949.
Devaskar, S., Chundu, K., Zahm, D.S., Holtzclaw, L., Holloran, K., 1992. The neonatal rabbit brain glucose transporter. Brain Res. Dev. Brain Res. 67, 95–103.
Devaskar, S.U., Rajakumar, P.A., Mink, R.B., McKnight, R.A., Thamotharan, S., Hicks, S. J., 1999. Effect of development and hypoxic-ischemia upon rabbit brain glucose transporter expression. Brain Res. 823, 113–128.
Dworschak, G.C., Draaken, M., Hilger, A.C., Schramm, C., Bartels, E., Schmiedeke, E., Grasshoff-Derr, S., Marzheuser, S., Holland-Cunz, S., Lacher, M., Jenetzky, E., Zwink, N., Schmidt, D., Nothen, M.M., Ludwig, M., Reutter, H., 2015. Genome-wide mapping of copy number variations in patients with both anorectal malformations and central nervous system abnormalities. Birth Defects Res A Clin Mol Teratol 103, 235–242.
Fung, C., Evans, E., Shin, D., Shin, B.C., Zhao, Y., Sankar, R., Chaudhuri, G., Devaskar, S. U., 2010. Hypoxic-ischemic brain injury exacerbates neuronal apoptosis and precipitates spontaneous seizures in glucose transporter isoform 3 heterozygous null mice. J. Neurosci. Res. 88, 3386–3398.
Ganguly, A., McKnight, R.A., Raychaudhuri, S., Shin, B.C., Ma, Z., Moley, K., Devaskar, S. U., 2007. Glucose transporter isoform-3 mutations cause early pregnancy loss and fetal growth restriction. Am. J. Physiol. Endocrinol. Metab. 292, E1241–E1255.
Gorski, J.A., Talley, T., Qiu, M., Puelles, L., Rubenstein, J.L., Jones, K.R., 2002. Cortical excitatory neurons and glia, but not GABAergic neurons, are produced in the Emx1-expressing lineage. J. Neurosci. 22, 6309–6314.
Jansch, C., Gunther, K., Waider, J., Ziegler, G.C., Forero, A., Kollert, S., Svirin, E., Puhringer, D., Kwok, C.K., Ullmann, R., Maierhofer, A., Flunkert, J., Haaf, T., Edenhofer, F., Lesch, K.P., 2018. Generation of a human induced pluripotent stem cell (iPSC) line from a 51-year-old female with attention-deficit/hyperactivity disorder (ADHD) carrying a duplication of SLC2A3. Stem Cell Res. 28, 136–140.
Leen, W.G., Wevers, R.A., Kamsteeg, E.J., Scheffer, H., Verbeek, M.M., Willemsen, M.A., 2013. Cerebrospinal fluid analysis in the workup of GLUT1 deficiency syndrome: a systematic review. JAMA Neurology 70, 1440–1444.
Lisman, J., Yasuda, R., Raghavachari, S., 2012. Mechanisms of CaMKII action in long-term potentiation. Nat. Rev. Neurosci. 13, 169–182.
Magistretti, P.J., Pellerin, L., 1999. Cellular mechanisms of brain energy metabolism and their relevance to functional brain imaging. Philos. Trans. R. Soc. Lond. Ser. B Biol. Sci. 354, 1155–1163.
Merikangas, A.K., Almasy, L., 2020. Using the tools of genetic epidemiology to understand sex differences in neuropsychiatric disorders. Genes Brain Behav 19, e12660.
Merker, S., Reif, A., Ziegler, G.C., Weber, H., Mayer, U., Ehlis, A.C., Conzelmann, A., Johansson, S., Muller-Reible, C., Nanda, I., Haaf, T., Ullmann, R., Romanos, M., Fallgatter, A.J., Pauli, P., Strekalova, T., Jansch, C., Vasquez, A.A., Haavik, J., Ribases, M., Ramos-Quiroga, J.A., Buitelaar, J.K., Franke, B., Lesch, K.P., 2017. SLC2A3 single-nucleotide polymorphism and duplication influence cognitive processing and population-specific risk for attention-deficit/hyperactivity disorder. J. Child Psychol. Psychiatry 58, 798–809.
Pearson, T.S., Akman, C., Hinton, V.J., Engelstad, K., De Vivo, D.C., 2013. Phenotypic spectrum of glucose transporter type 1 deficiency syndrome (Glut1 DS). Current Neurology and Neuroscience Reports 13, 342.
Roeske, D., Ludwig, K.U., Neuhoff, N., Becker, J., Bartling, J., Bruder, J., Brockschmidt, F.F., Warnke, A., Remschmidt, H., Hoffmann, P., Muller-Myhsok, B., Nothen, M.M., Schulte-Korne, G., 2011. First genome-wide association scan on neurophysiological endophenotypes points to trans-regulation effects on SLC2A3 in dyslexic children. Mol. Psychiatry 16, 97–107.
Shah, K., Desilva, S., Abbruscato, T., 2012. The role of glucose transporters in brain disease: diabetes and Alzheimer's disease. Int. J. Mol. Sci. 13, 12629–12655.
Sharma, S.R., Gonda, X., Tarazi, F.I., 2018. Autism Spectrum disorder: classification, diagnosis and therapy. Pharmacol. Ther. 190, 91–104.
Shin, B.C., Cepeda, C., Estrada-Sanchez, A.M., Levine, M.S., Hodaei, L., Dai, Y., Jung, J., Ganguly, A., Clark, P., Devaskar, S.U., 2018. Neural deletion of glucose transporter isoform 3 creates distinct postnatal and adult neurobehavioral phenotypes. J. Neurosci. 38, 9579–9599.
Stibbe, T., Huang, J., Paucke, M., Ulke, C., Strauss, M., 2020. Gender differences in adult ADHD: cognitive function assessed by the test of attentional performance. PLoS One 15, e0240810.
Stocker, A.M., O'Leary, D.D., 2016. Emx1 is required for neocortical area patterning. PLoS One 11, e0149900.
Szablewski, L., 2017. Glucose transporters in brain: in health and in Alzheimer's disease. J. Alzheimers Dis. 55, 1307–1320.
Takata, K., Hirano, H., Kasahara, M., 1997. Transport of glucose across the blood-tissue barriers. Int. Rev. Cytol. 172, 1–53.
Uldry, M., Thorens, B., 2004. The SLC2 family of facilitated hexose and polyol transporters. Pflugers Arch. 447, 480–489.
Veal, C.D., Reekie, K.E., Lorentzen, J.C., Gregersen, P.K., Padyukov, L., Brookes, A.J., 2014. A 129-kb deletion on chromosome 12 confers substantial protection against rheumatoid arthritis, implicating the gene SLC2A3. Hum. Mutat. 35, 248–256.
Wang, D., Pascual, J.M., Yang, H., Engelstad, K., Jhung, S., Sun, R.P., De Vivo, D.C., 2005. Glut-1 deficiency syndrome: clinical, genetic, and therapeutic aspects. Ann. Neurol. 57, 111–118.
Weisova, P., Concannon, C.G., Devocelle, M., Prehn, J.H., Ward, M.W., 2009. Regulation of glucose transporter 3 surface expression by the AMP-activated protein kinase mediates tolerance to glutamate excitation in neurons. J. Neurosci. 29, 2997–3008.
Zalcman, G., Federman, N., Romano, A., 2018. CaMKII isoforms in learning and memory: localization and function. Front. Mol. Neurosci. 11, 445.
Zhao, Y., Fung, C., Shin, D., Shin, B.C., Thamotharan, S., Sankar, R., Ehninger, D., Silva, A., Devaskar, S.U., 2010. Neuronal glucose transporter isoform 3 deficient mice demonstrate features of autism spectrum disorders. Mol. Psychiatry 15, 286–299.
Ziegler, G.C., Almos, P., McNeill, R.V., Jansch, C., Lesch, K.P., 2020. Cellular effects and clinical implications of SLC2A3 copy number variation. J. Cell. Physiol. 235, 9021–9036.
Zovein, A., Flowers-Ziegler, J., Thamotharan, S., Shin, D., Sankar, R., Nguyen, K., Gambhir, S., Devaskar, S.U., 2004. Postnatal hypoxic-ischemic brain injury alters mechanisms mediating neuronal glucose transport. Am J Physiol Regul Integr Comp Physiol 286, R273–R282.